Suppporting Information for

Oxygen-independent Photonuclease activity of a new iron(II) complex

Bernardo de Souza, Fernando R. Xavier, Rosely A. Peralta, Adailton J. Bortoluzzi, Gilmar Conte, Hugo Gallardo, Franciele L. Fischer, Giselle Bussi, Hernán Terenzi* Ademir Neves.

Synthesis of complex **1**.

The complex **1** . 2DMSO was obtained by the addition of 1.5 mmol (0.38g) of the ligand and 0.5 mmol (0.36g) of $Fe(ClO_4)_2.6H_2O$ in 30 mL of dimethylsulfoxide at 60ºC under magnetic stirring. Tetrabutylammonium hexafluorophosphate (1 mmol, 0.39g) was added and solution stirred over 20 minutes where the resulting mixture was cooled at room temperature and filtered. Dark red single crystals suitable for X ray analysis. of the Fe^{II} complex were obtained several days later, at the room temperature (the selected bond lengths and angles have been placed in supporting information). Elemental analysis calculated for $C_{40}H_{30}F_{12}FeN_{12}O_2P_2S_5$, fw = 1216.85 g.mol^{-1}: C, 39.48; H, 2.48; N, 13.81; S, 13.17. Found C, 39.28; H, 2.46; N, 13.74; S, 13.10 %. IR (cm^{-1}):3080 [ν(C-H)$_{ar}$]; 2970, 2880 [ν(C-H)$_{aliph}$]; 1628, 1467, 1399, [ν(C=C) and (C=N)]; 1090 [ν(S=O)$_{DMSO}$]; 841 [ν(P-F)$_{PF6}$]; 731 [δ(C-H)]; 554 [ν(C-S)$_{DMSO}$].

Crystallography

A red plate crystal was selected from the crystalline sample of complex **1**, it was handled with protective oil to prevent solvent loss and sealed in a glass capillary. Crystallographic data were measured on an Enraf-Nonius CAD4 diffractometer with graphite monochromated Mo-Ka radiation using ω-2θ scan method, at room temperature. Cell parameters were determined from 25 centered reflections in the θ range 3.98-15.95^o and were refined by least squares method. Intensity was controlled by using three standard reflections, which were measured at regular intervals, and no significant loss of intensity was observed during the data collection. The collected intensities were corrected for the Lorentz and for polarization effects. A semi-empirical absorption correction (psi-scan) was also applied to all intensities. The structure was solved by direct methods and was refined by the full-matrix least-squares method. All non-hydrogen atoms were refined with anisotropic displacement parameters. Hydrogen atoms were placed at idealized positions using standard geometric criteria. Both PF_6^- anions are disordered and the fluorine atoms occupy two alternative positions.

Table 1. Crystal data and structure refinement for complex **1**.

Empirical formula	$C_{40}H_{30}F_{12}FeN_{12}O_2P_2S_5$	
Formula weight	1216.85	
Temperature	293(2) K	
Wavelength	0.71069 Å	
Crystal system	Triclinic	
Space group	$P\bar{1}$	
Unit cell dimensions	a = 12.097(1) Å	α = 81.74(1)°.
	b = 12.390(1) Å	β = 77.95(1)°.
	c = 16.561(3) Å	γ = 79.67(1)°.
Volume	2373.6(5) $Å^3$	
Z	2	
Density (calculated)	1.703 Mg/m^3	
Absorption coefficient	0.705 mm^{-1}	
F(000)	1228	
Crystal size	0.33 x 0.30 x 0.03 mm^3	
Theta range for data collection	1.26 to 25.07°.	
Index ranges	$-14 \le h \le 14$, $-14 \le k \le 14$, $-19 \le l \le 0$	
Reflections collected	8654	
Independent reflections	8339 (R_{int} = 0.0268)	
Absorption correction	Psi-scan	
Max. and min. transmission	0.973 and 0.801	
Refinement method	Full-matrix least-squares on F^2	
Data / restraints / parameters	8339 / 690 / 777	
Goodness-of-fit on F^2	1.031	
Final R indices [$I>2\sigma(I)$]	R_1 = 0.0536, wR_2 = 0.1225	
R indices (all data)	R_1 = 0.1381, wR_2 = 0.1467	
Largest diff. peak and hole	0.510 and -0.452 e.$Å^{-3}$	

Table S1. Selected bond lengths [Å] and angles [º] for complex **1**.

Fe1-N1	1.962(4)	N10-S11	1.624(6)
Fe1-N21	1.969(4)	S11-N12	1.634(6)
Fe1-N44	1.971(4)	N30-S31	1.617(5)
Fe1-N4	1.973(4)	S31-N32	1.623(5)
Fe1-N41	1.976(4)	N50-S51	1.626(4)
Fe1-N24	1.997(4)	S51-N52	1.618(5)
N1-Fe1-N21	175.00(16)	N4-Fe1-N24	90.77(15)
N1-Fe1-N44	91.31(16)	N41-Fe1-N24	93.57(15)
N21-Fe1-N44	92.45(16)	N44-Fe1-N24	173.43(16)
N1-Fe1-N4	82.64(17)	N4-Fe1-N41	174.83(16)
N21-Fe1-N4	93.83(16)	N1-Fe1-N24	94.11(16)
N44-Fe1-N4	93.59(16)	N21-Fe1-N24	82.36(16)
N1-Fe1-N41	94.24(16)	N44-Fe1-N41	82.33(15)
N21-Fe1-N41	89.53(16)		

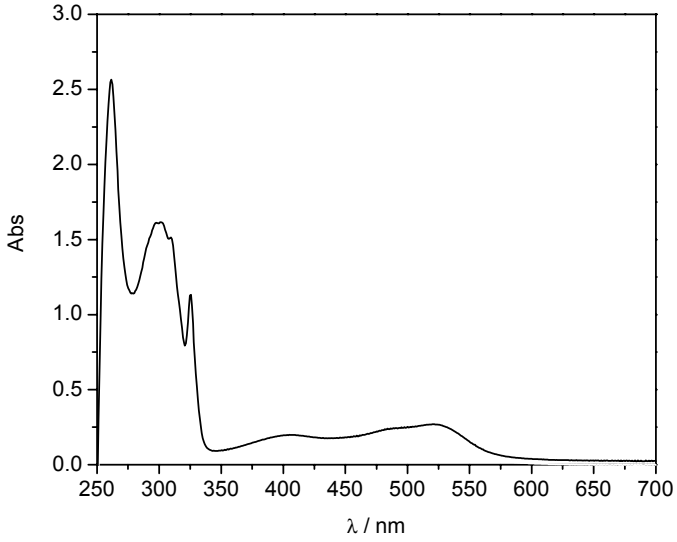

Figure S1. Electronic spectrum of **1** in DMSO/H_2O 1:3 v/v. [complex] = 4.33 x 10^{-5} mol.L^{-1}.

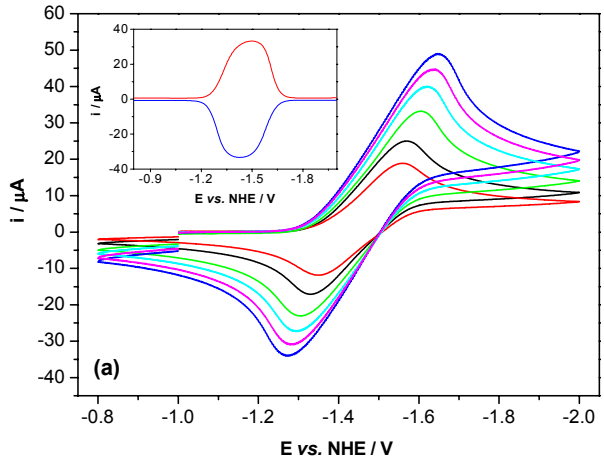

Figure S2. Cyclic and square wave (inset) voltammograms of the ligand in DMSO solution. Scan rates: 50 – 100 $mV.s^{-1}$ for CV and 15 mV; 30 Hz for SW, respectively. Supporting electrolyte: 0.1 $mol.L^{-1}$ *n*-$BuNPF_6$. Three-electrode electrochemical cell: Pt (working); Ag/Ag^{+} (reference) and Pt wire (auxiliary).

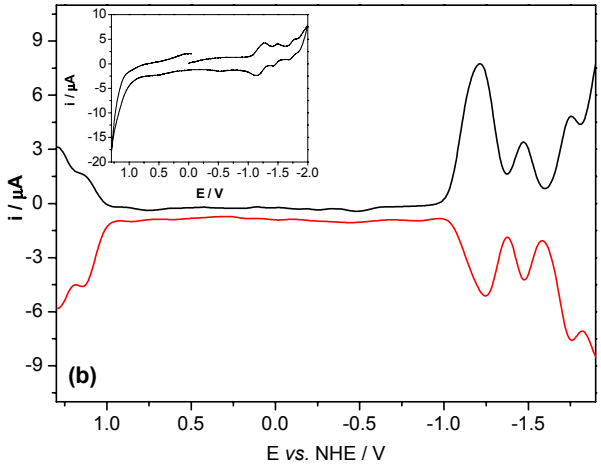

Figure S3. Square wave and cyclic (inset) voltammograms of complex 1 in DMSO solution. Scan rates: 15 mV; 30 Hz for SW and 300 $mV.s^{-1}$ for CV, respectively. Supporting electrolyte: 0.1 $mol.L^{-1}$ *n*-$BuNPF_6$. Three-electrode electrochemical cell: Pt (working); Ag/Ag^{+} (reference) and Pt wire (auxiliary).

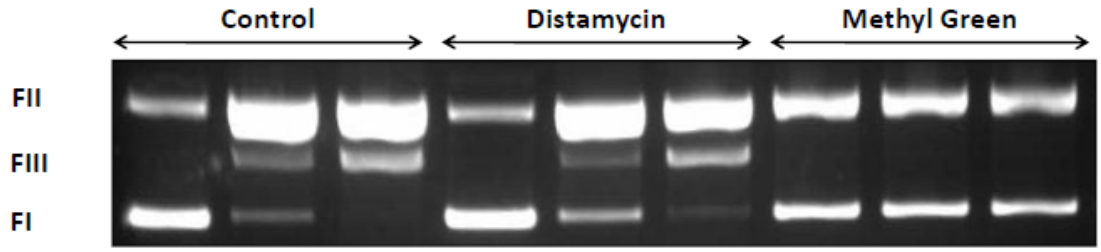

Lanes	1	2	3	4	5	6	7	8	9
FII (%)	0.0	82.3	79.6	0.0	69.4	75.2	0.0	0.4	0.0
FIII(%)	0.0	4.7	20.4	0.0	3.0	20.6	0.0	0.0	0.0
FI (%)	100.0	12.9	0.0	100.0	27.6	4.1	100.0	99.6	100.0

Figure S4. Influence of DNA groove-binders (50 $\mu molL^{-1}$) on DNA cleavage activity of **1**. Lanes 1, 2 and 3: DNA control, DNA + **1** (4 $\mu molL^{-1}$) and DNA + **1** (6 $\mu molL^{-1}$), respectively; Lanes 4, 5 and 6: DNA control + Distamycin, DNA + **1** (4 $\mu molL^{-1}$) + Distamycin and DNA + **1** (6 $\mu molL^{-1}$) + Distamycin, respectively; Lanes 7, 8 and 9: DNA control + Methyl Green, DNA + **1** (4 $\mu molL^{-1}$) + Methyl Green and DNA + **1** (6 $\mu molL^{-1}$) + Methyl Green, respectively. All reactions were carried out in 25 $mmolL^{-1}$ PIPES, pH 7.0 and DMSO/H2O (25% v/v) and incubated for 5 min under a UV light (365 nm) at room temperature.

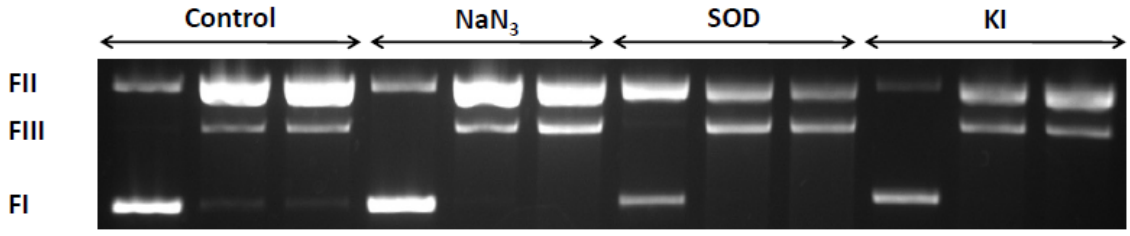

Lanes	1	2	3	4	5	6	7	8	9	10	11	12
FII (%)	0.0	82.4	79.6	0.0	80.5	68.9	0.0	57.3	50.1	0.0	67.2	76.6
FIII (%)	0.0	12.4	16.2	0.0	19.5	31.1	0.0	42.7	49.9	0.0	32.8	23.4
FI (%)	100.0	5.3	4.2	100.0	0.0	0.0	100.0	0.0	0.0	100.0	0.0	0.0

Figure S5. DNA photocleavage activity of **1** in the absence (lanes 1-3) or presence (lanes 4-12) of different inhibitors of reactive oxygen species (ROS). Reactions were performed in 25 $mmolL^{-1}$ PIPES, pH 7.0 in DMSO/H_2O (25% v/v) and incubated for 5 min under a UV light at room temperature. Lanes 1, 4, 7 and 10: DNA controls; Lanes 2, 5, 8 and 11: DNA + **1** (4 $\mu molL^{-1}$); Lanes 3, 6, 9 and 12: DNA + **1** (6 $\mu molL^{-1}$). The inhibitors used were: Lanes 4-6: NaN_3 (500 $\mu molL^{-1}$); Lanes: 7-9: SOD (15 units in a final volume reaction of 20 $\mu molL^{-1}$); Lanes 10-12: KI (500 $\mu molL^{-1}$).

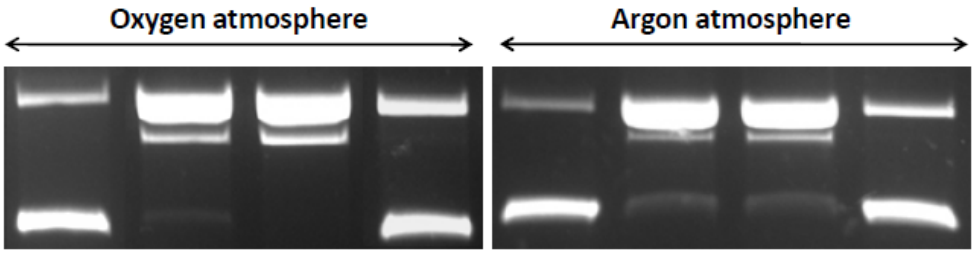

Lanes	1	2	3	4	5	6	7	8
FII (%)	0.0	76.4	75.2	23.3	0.0	79.0	74.2	4.6
FIII (%)	0.0	20.1	24.8	0.0	0.0	10.2	16.3	0.0
FI (%)	100.0	3.5	0.0	76.7	100.0	10.8	9.5	95.4

Figure S6. Photocleavage of pBSK II (25 μmol^{-1} pb) by **1** in 25 $mmol^{-1}$ PIPES, pH 7.0 in H_2O/DMSO (3:1 v/v). Lanes 1-4: Reactions in oxygen atmosphere; Lanes 5-8: Reactions in Argon atmosphere. Lanes 1 and 5: DNA controls; Lanes 2 and 6: DNA + **1** (4 $\mu molL^{-1}$); Lanes 3 and 7: DNA + **1** (6 $\mu molL^{-1}$) and Lanes 4 and 8: 400 μmol^{-1} Fe-EDTA + 40 $\mu molL^{-1}$ DTT. Incubation: UV light (365 nm) for 5 min at room temperature + 30 min in dark conditions at 37

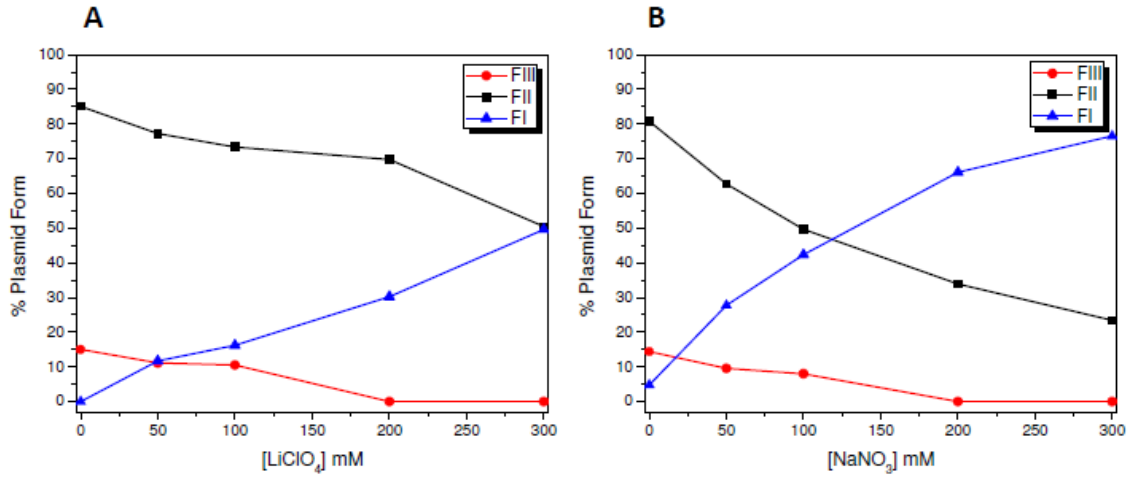

Figure S7. Effect of ionic strength on supercoiled plasmid DNA photocleavage by **1**. Reaction conditions: 25 $mmolL^{-1}$ PIPES, pH 7.0, DMSO/H_2O (25% v/v). Incubation: UV light (365 nm) for 5 min at room temperature.

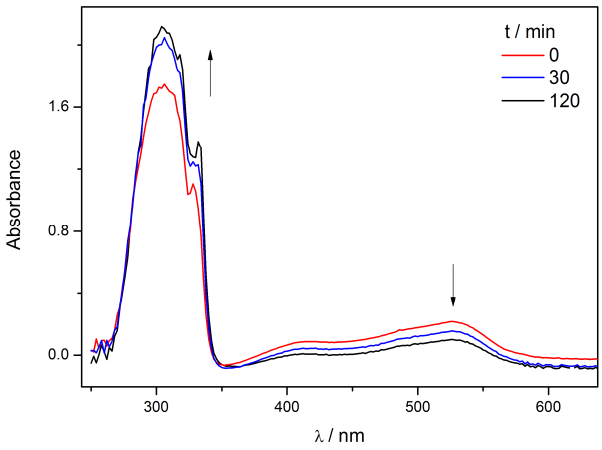

Figure S8. Spectra recorded after 365 nm irradiation for several minutes. [complex] = 2 x 10^{-5} mol.L^{-1}

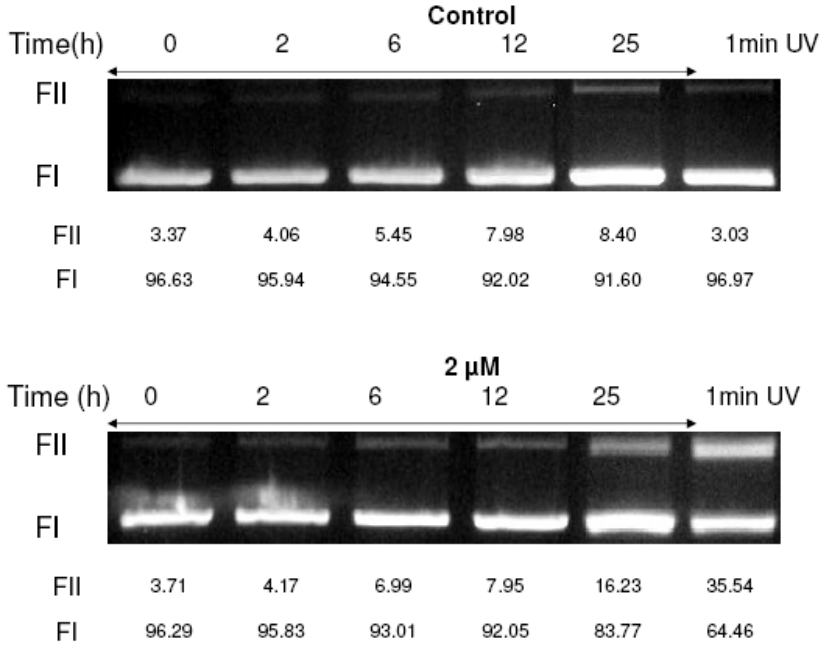

Figure S9. Photocleavage of pBSK II (25 µmol^{-1} pb) by **1** in 25 mmol^{-1} PIPES, pH 7.0 in H_2O/DMSO (3:1 v/v). The experiments were performed in dark, at the absence and presence of the complex and within one minute of UV light exposure, indicating that the complex is ~ 6000 more active when exposed to light.